ORGANIC CHEMISTRY

10.1126/sciadv.1500656

Copper-catalyzed aerobic oxidative coupling: From ketone and diamine to pyrazine

Kun Wu,[1]* Zhiliang Huang,[1,2]* Xiaotian Qi,[3] Yingzi Li,[3] Guanghui Zhang,[1,2] Chao Liu,[1] Hong Yi,[1] Lingkui Meng,[1] Emilio E. Bunel,[2] Jeffrey T. Miller,[2] Chih-Wen Pao,[4] Jyh-Fu Lee,[4] Yu Lan,[3†] Aiwen Lei[1,2,5†]

Copper-catalyzed aerobic oxidative C–H/N–H coupling between simple ketones and diamines was developed toward the synthesis of a variety of pyrazines. Various substituted ketones were compatible for this transformation. Preliminary mechanistic investigations indicated that radical species were involved. X-ray absorption fine structure experiments elucidated that the Cu(II) species 5 coordinated by two N atoms at a distance of 2.04 Å and two O atoms at a shorter distance of 1.98 Å was a reactive one for this aerobic oxidative coupling reaction. Density functional theory calculations suggested that the intramolecular coupling of cationic radicals was favorable in this transformation.

INTRODUCTION

Oxidative cross-coupling reactions have recently shown great potential in carbon-carbon and carbon-heteroatom bond formation (*1*–*4*). Generally, organometallic compounds (R–M) can be used as one of the reaction partners in these transformations, but alcohols, amines, and hydrocarbons (R–H) can be directly used as well (*5*–*13*). Compared with R–M, R–H is an "ideal" reactant in view of atom-economical synthesis. Up to now, seeking and applying different R–H in oxidative C–H/C–H or C–H/Y–H (Y = N, O, S, etc.) coupling reactions remains a challenge.

Pyrazine, which is one of the well-known and important classes of heterocyclic compounds, exhibits extraordinary biological and pharmaceutical properties (*14*–*18*). In recent years, pyrazines have received a lot of attention because of their applications in the field of luminescent materials (*19*). Therefore, exploring effective methods toward the synthesis of pyrazines is appealing and important. Traditionally, condensation of α-diketone and diamine is a predominant method for the construction of pyrazines (Scheme 1, Path A) (*20*–*25*). Most α-diketones are often not commercially available, and the preparation processes are energy-consuming and complicated (*26*–*28*). Hence, if simple ketones could be applied instead of α-diketones in this synthesis, it would be a more attractive strategy to access pyrazines (Scheme 1, Path B).

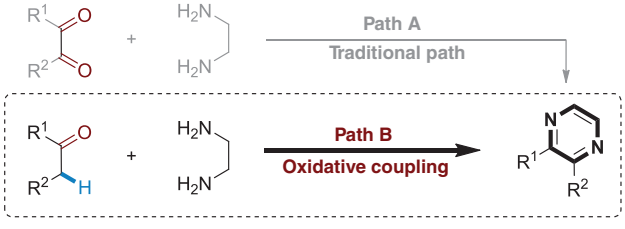

Scheme 1. Traditional and theoretical pathways for the synthesis of pyrazines.

A C–N bond formation involving the α-C–H of ketones and N–H of primary amines is required to realize the designed transformation. Both are known nucleophiles and cannot directly react to form C–N bonds. There are some clues in the literature regarding the C–N bond formation involving a Csp^3–H and an N–H under oxidative conditions (*29*–*37*). However, to the best of our knowledge, only a few examples in which I_2, *N*-bromosuccinimide, or hypervalent iodine was used as oxidant were developed to construct the C–N bond by using α-C–H of simple ketones and N–H of primary amines (*38*–*41*). Herein, we proposed a strategy (Scheme 2) to achieve this transformation by utilizing copper salt as the catalyst and O_2 as the oxidant. Initially, a primary amine was introduced to react with ketone to produce imine **1A** (*42*), which could isomerize to enamine **2A** (*43*, *44*). The isomer might be oxidized by losing one electron in the presence of a catalyst [Cu(II)] and an oxidant (O_2) to form enamine radical cation **3A** (*45*, *46*). As a relatively electron-deficient species, **3A** might be attacked by nucleophiles (N–H) (*47*, *48*). After losing another electron, the bond formation between α-C–H of ketones and N–H of primary amines could be realized. In this regard, we attempt to demonstrate an oxidative coupling between ketones and diamines toward the synthesis of pyrazines by single electron transfer.

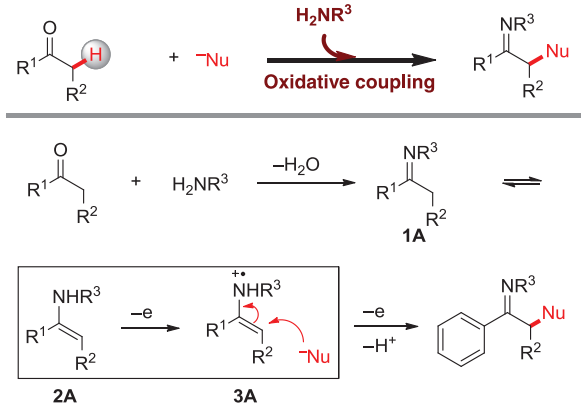

Scheme 2. The proposed strategy for oxidative coupling reactions between simple ketones and nucleophiles.

RESULTS AND DISCUSSION

The density functional theory (DFT) method B3LYP was initially performed to further analyze the practicality of our proposed strategy

[1]College of Chemistry and Molecular Sciences, Institute for Advanced Studies, Wuhan University, Wuhan 430072, China. [2]Chemical Sciences and Engineering Division, Argonne National Laboratory, 9700 South Cass Avenue, Argonne, IL 60439, USA. [3]School of Chemistry and Chemical Engineering, Chongqing University, Chongqing 400030, China. [4]National Synchrotron Radiation Research Center, Hsinchu 30076, Taiwan. [5]National Research Center for Carbohydrate Synthesis, Jiangxi Normal University, Nanchang 330022, China.
*These authors contributed equally to this work.
†Corresponding author. E-mail: aiwenlei@whu.edu.cn (A.L.); lanyu@cqu.edu.cn (Y.L.)

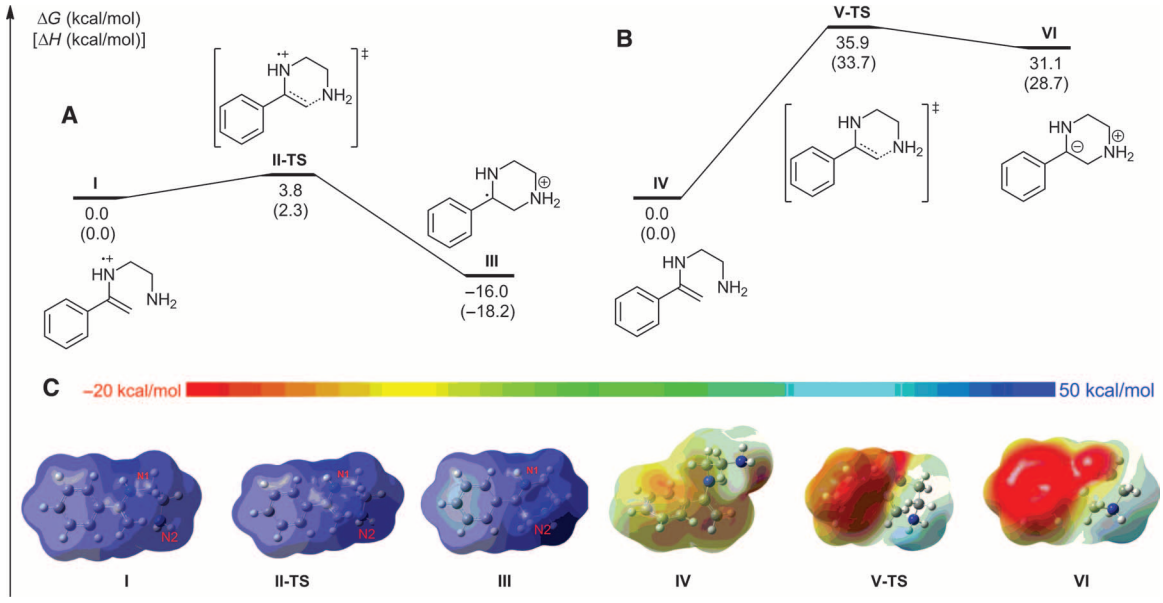

Fig. 1. Density functional theory (DFT) calculations for energy comparisons. (**A** to **C**) Free energy profile for the intramolecular cyclization process (A and B), and the corresponding electrostatic potential (ESP) maps (C).

(*49*). As illustrated in Fig. 1A, the nucleophilic addition of cationic radical **I** takes place via transition state **II-TS** with only a 3.8-kcal/mol barrier, after which the generated cationic radical **III** (16.0 kcal/mol) becomes more stable than cationic radical **I.** As a comparison, the corresponding cyclization of neutral enamine **IV** has also been calculated. The free energy profile (Fig. 1B) shows that the activation free energy of intramolecular cyclization via transition state **V-TS** is 35.9 kcal/mol, which is 32.1 kcal/mol higher than that of cationic radical **I.** The relative free energy of the formed complex **VI** is 31.1 kcal/mol higher than that of complex **IV.** The calculated ESP (Fig. 1C) could rationalize this difference. From the ESP results, the cyclization from **I** to **III** is a charge transfer process, whereas that from **IV** to **VI** is a charge separation process. The latter is much more difficult than the former; that is, oxidative coupling between ketones and diamines toward the synthesis of pyrazines by single electron transfer is much more facile.

On the basis of the DFT calculations, the C–N bond formation reaction of acetophenone **1a** and ethylenediamine **2a** toward the synthesis of pyrazine was commenced by using 30 mol% of copper(I) iodide as the catalyst and O_2 as the oxidant, because these reaction parameters are standard for the formation of radical cations (*42*, *50*, *51*). After several potential solvents were evaluated, dimethyl acetamide (DMA)/Et_3N (2:1) proved to be the most effective, and the corresponding pyrazine product was obtained in moderate yield (Table 1, entry 1). Various additives were also examined (Table 1, entries 2 to 4). The efficiency of the reaction was significantly improved by the addition of the inexpensive and readily available lithium chloride (Table 1, entry 5). In addition, CuI plays a critical role in the reaction with only trace amounts of **3a** formed in its absence (Table 1, entry 13). Other copper salts, such as CuCl, CuBr, $CuCl_2$, and $Cu(OTf)_2$, were less effective (Table 1, entries 6 to 9). The reaction also took place efficiently with lower loadings of CuI (Table 1, entries 10 to 12). When DMA was used as the sole solvent, the yield of the desired product was slightly lower (Table 1, entry 14). Finally, the reaction conditions described in entry 11 were selected as the standard conditions for further investigations.

Table 1. Impact of reaction parameters on oxidative C–H/N–H coupling reaction. For more details on metals, solvents, temperature, ratio of substrates, and the amount of LiCl, see tables S1 to S5.

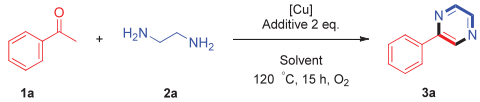

Entry	[Cu](equiv)	Additive	Solvent	3a*[%]
1	CuI(0.3)	---	DMA/Et_3N(2:1)	55
2	CuI(0.3)	LiBr	DMA/Et_3N(2:1)	60
3	CuI(0.3)	KI	DMA/Et_3N(2:1)	78
4	CuI(0.3)	ZnCl2	DMA/Et_3N(2:1)	74
5	CuI(0.3)	LiCl	DMA/Et_3N(2:1)	79(74)
6	CuCl(0.3)	LiCl	DMA/Et_3N(2:1)	37
7	CuBr(0.3)	LiCl	DMA/Et_3N(2:1)	36
8	$CuCl_2$(0.3)	LiCl	DMA/Et_3N(2:1)	17
9	$Cu(OTf)_2$(0.3)	LiCl	DMA/Et_3N(2:1)	5
10	CuI(0.2)	LiCl	DMA/Et_3N(2:1)	80(74)
11	CuI(0.1)	LiCl	DMA/Et_3N(2:1)	78(75)
12	CuI(0.05)	LiCl	DMA/Et_3N(2:1)	68
13	---	LiCl	DMA/Et_3N(2:1)	<1
14	CuI(0.3)	LiCl	DMA	60

*Gas chromatography yield based on **1a** with biphenyl used as the internal standard.

To further investigate the scope of this catalytic system, we used a variety of aryl methyl ketones to couple with ethylenediamine **2a** under the optimized reaction conditions (Table 2). All substrates proceeded well and afforded corresponding products in moderate to good yields. Aryl methyl ketones with an electron-donating group (OMe) or an electron-withdrawing group (CN, CF_3) could react with **2a** smoothly to afford the desired products in moderate to good yields (Table 2, entries 5 and 10 to 13). Acetophenones with halogen substituents (F, Cl, and Br) were also suitable substrates to yield the corresponding

Table 2. Copper-catalyzed oxidative C–H/N–H coupling of aryl ketone and 2a.

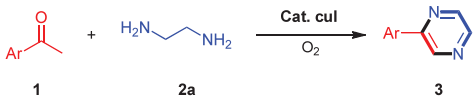

1 2a 3

Entry	Substrate 1	Product 3	Yield*
1	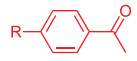	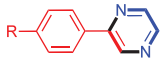	R = H, **3a:** 75%
2			R = Ph, **3b:** 71%
3			R = F, **3c:** 38%†
4			R = Br, **3d:** 60%
5			R = CN, **3e:** 65%†
6	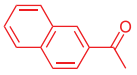	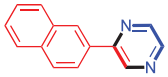	**3f:** 75%
7	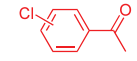	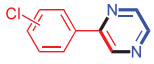	**3g:** 2-Cl, 56%
8			**3h:** 3-Cl, 72%†
9			**3i:** 4-Cl, 70%
10	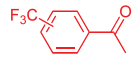	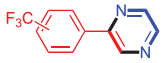	**3j:** 3-CF_3, 67%
11			**3k:** 4-CF_3, 68%
12	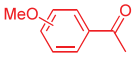	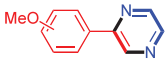	**3l:** 3-OMe,56%
13			**3m:** 4-OMe,66%†
14	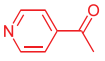	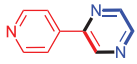	**3n:** 72%
15	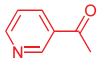	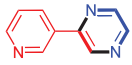	**3o:** 71%
16		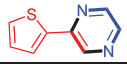	**3p:** 60%

*Conditions: **1** (0.5 mmol), **2a** (2.5 mmol), CuI (0.05 mmol), LiCl (1.0 mmol), DMA/Et_3N = 2:1 (1.5 ml), 120°C, 15 hours, under O_2 (1 atm). Isolated yields. †Twenty-four hours.

Table 3. Copper-catalyzed oxidative C–H/N–H coupling of other ketones and 2a. For more attempts between other ketones and ethylenediamine, see table S6.

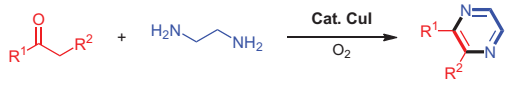

1 2a 3

Entry	Substrate 1	Product 3	Yield*
1	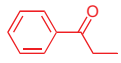	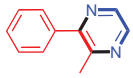	**3q:** 60%
2	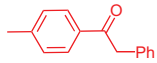	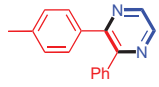	**3r:** 65%
3	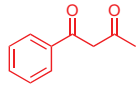	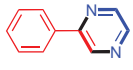	**3a:** 71%†
4	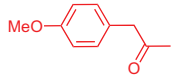	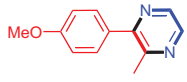	**3t:** 30%
5	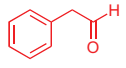	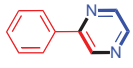	**3a:** 44%
6		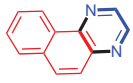	**3v:** 40%†
7		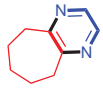	**3w:** 18%‡
8		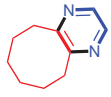	**3x:** 21%‡
9		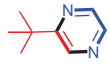	**3y:** 7%‡,‖

*Conditions: **1** (0.5 mmol), **2a** (2.5 mmol), CuI (0.05 mmol), LiCl (1.0 mmol), DMA/Et_3N = 2:1 (1.5 ml), 120°C, 15 hours, under O_2 (1 atm). Isolated yields. †Twenty-four hours. ‡CuI (30 mol%). ‖Nuclear magnetic resonance yield.

products, which enabled a potential application for further functionalization (Table 2, entries 3, 4, and 7 to 9). 1-([1,1′-Biphenyl]-4-yl)ethanone and 1-(naphthalen-2-yl)ethanone were also suitable substrates for this transformation (Table 2, entries 2 and 6). In addition, heterocyclic methyl ketones could react well with **2a** to give the corresponding products in good yields (Table 2, entries 14 to 16).

In addition to aryl methyl ketones, various other ketones were also reacted with **2a**, and the results are given in Table 3. The reaction between **2a** and propiophenone or 2-phenyl-1-(*p*-tolyl)ethanone proceeded to give the desired products in good yields (Table 3, entries 1 and 2). For the reaction of 1-phenylbutane-1,3-dione with **2a**, **3a** was obtained in 71% yield (Table 3, entry 3). In this reaction, C–C bond cleavage also occurred. The reaction of 1-(4-methoxyphenyl)propan-2-one with 2-phenylacetaldehyde produced the pyrazine ring as well (Table 3, entries 4 and 5). 3,4-Dihydronaphthalen-1(2*H*)-one was suitable for this reaction, generating benzo[*f*]quinoxaline in 40% yield (Table 3, entry 6). The reactions of **2a** with simple alkyl ketones, such as cycloheptanone, cyclooctanone, and 3,3-dimethylbutan-2-one, proceeded to afford the desired pyrazines (Table 3, entries 7 to 9).

As shown in Table 4, various diamines other than **2a** also gave pyrazine products in this copper-catalyzed aerobic oxidative C–H/N–H coupling reaction. For example, 1,2-diphenylethane-1,2-diamine reacted with acetophenone, 1-(4-chlorophenyl)ethan-1-one, and propiophenone to afford the corresponding products in moderate yields (Table 4, entries 1 to 3). The reaction of propane-1,2-diamine with acetophenone gave two products in 43 and 29% yields (Table 4, entry 4). In addition, when other unsymmetrical 1,2-diamines were used with **1a**, a similar selectivity was obtained (Table 4, entries 5 and 6).

As proposed, the copper-catalyzed aerobic oxidative C–H/N–H cross-coupling might undergo a radical process. To investigate this possibility, we performed a radical-trapping experiment. In the presence of 1 eq of 2,6-bis(1,1-dimethylethyl)-4-methylphenol, no product **3a** was obtained under the standard conditions (see Supporting Information, scheme S3). The reaction between acetophenone (**1a**) and ethylenediamine (**2a**) was also monitored by electron paramagnetic resonance (EPR), and the results are shown in Fig. 2. Cu(II) signal was detected during the reaction (Fig. 2A) (*52*, *53*). In addition, when 5,5-dimethyl-1-pyrroline *N*-oxide (DMPO) was added to the reaction, the signal corresponding to DMPO–O(H) was identified (Fig. 2B), which is seen as four classical

Table 4. Copper-catalyzed oxidative C–H/N–H coupling of 1 and 2.

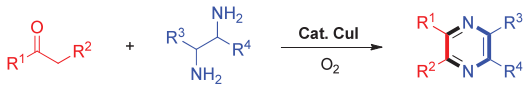

1 2 4

Entry	Product*	Entry	Product*
1	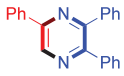 **4a:** 66%	2	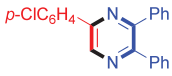 **4b:** 66%
3	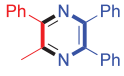 **4c:** 58%	4	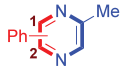 **4d:** 72%, 60:40 (1/2)
5	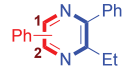 **4e:** 60%, 62:38 (1/2)	6	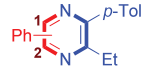 **4f:** 62%, 65:35 (1/2)

*Conditions: **1** (0.5 mmol), **2** (2.5 mmol), CuI (0.05 mmol), LiCl (1.0 mmol), DMA/Et_3N = 2:1 (1.5 ml), 120°C, 15 hours, under O_2 (1 atm). Isolated yields.

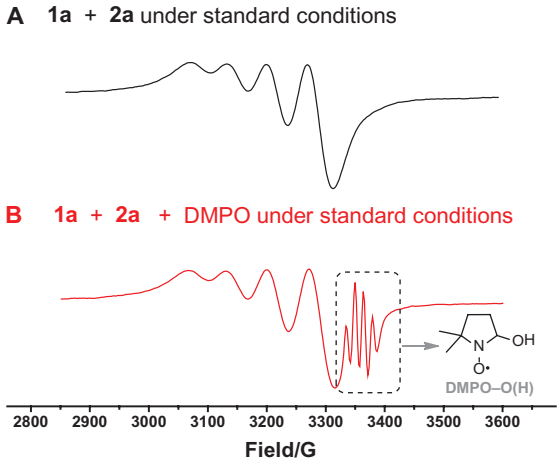

Fig. 2. The capture experiment of hydroxyl radical. (**A** and **B**) The EPR spectra (X band, 9.4 GHz, room temperature) of (A) the reaction mixture of **1a** and **2a** under standard conditions and (B) the reaction mixture of **1a** and **2a** with the addition of DMPO under standard conditions.

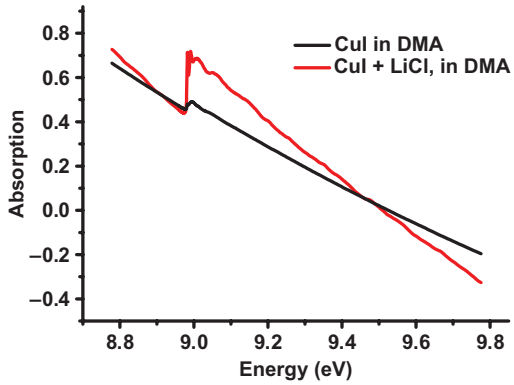

Fig. 3. Copper K-edge spectrum (black line, 0.6 mmol of CuI in 12 ml of DMA; red line, 0.6 mmol of CuI and 12 mmol of LiCl in 12 ml of DMA).

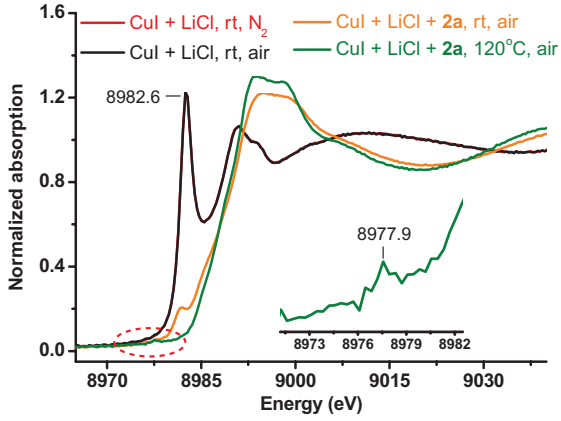

Fig. 4. XANES spectra [red line, 0.6 mmol of CuI and 12 mmol of LiCl in 12 ml of DMA at room temperature (rt) under N_2 for 5 min; black line, 0.6 mmol of CuI and 12 mmol of LiCl in 12 ml of DMA at rt under air for 5 min; brown line, 0.6 mmol of CuI, 12 mmol of LiCl, and 30 mmol of 2a in 12 ml of DMA at rt under air for 5 min; green line, 0.6 mmol of CuI, 12 mmol of LiCl, and 30 mmol of 2a in 12 ml of DMA at 120°C under air for 5 min].

peaks (*54*–*56*). The calculated hyperfine splittings are g_0 (2.0069), α^H (14.9 G), and α^N (14.5 G). This result suggests that a hydroxyl radical may be involved in this transformation.

To further elucidate the mechanism, we performed experiments using x-ray absorption fine structure (XAFS) spectroscopy. As illustrated in Fig. 3, the DMA solution of CuI with LiCl and that without LiCl were tested. In the presence of LiCl, the edge step of copper K-edge spectrum is 0.31; however, it is only 0.05 without LiCl. Because the edge step is linearly proportional to the concentration of copper species, LiCl increases the solubility of CuI in DMA. We do observe that the turbid DMA solution of CuI became clear after the addition of LiCl, which is consistent with the XAFS.

The oxidation of Cu(I) to Cu(II) was also studied. As shown in Fig. 4, under N_2 or air, the XANES (x-ray absorption near-edge structure) spectrum of the mixture of CuI, LiCl, and DMF displays a peak at 8982.6 eV, which is assigned to a 1s → 4p Cu(I) transition. Upon addition of **2a**, Cu(I) is oxidized to Cu(II) by air at room temperature (partially oxidized) or at 120°C (completely oxidized in 5 min) as evidenced by the decrease in the Cu(I) pre-edge and a shift in the edge-energy position to 8984.9 eV. The small pre-edge peak at 8977.9 eV is also consistent with Cu(II) (Fig. 4, green line) (*57*, *58*). These results are consistent with the coordination of **2a** to Cu(I), increasing the electron density of the copper center, which then facilitates this oxidation.

The reactivity of this Cu(II) intermediate was also investigated (*59*–*63*). As illustrated in Scheme 3, when the Cu(II) was used in the oxidative C–H/N–H coupling reaction, the desired product could be obtained in 62% yield. The results indicated that the Cu(II) species obtained by oxidizing the mixture of CuI, LiCl, **2a**, and DMA with air or O_2 was active for the oxidative C–H/N–H coupling reaction.

The structure of this active Cu(II) was determined by fitting of the EXAFS data. As shown in Fig. 5, the Fourier transform of the raw EXAFS data and the obtained EXAFS fit for the first shell data are given. The

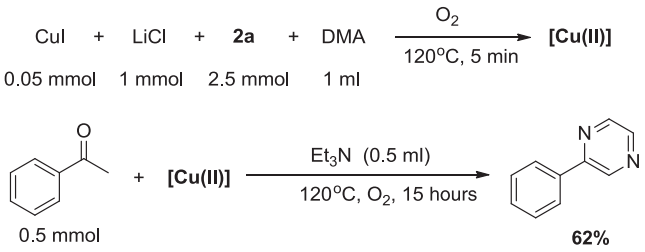

Scheme 3. Reactivity of the Cu(II) species in the oxidative C–H/N–H coupling reaction.

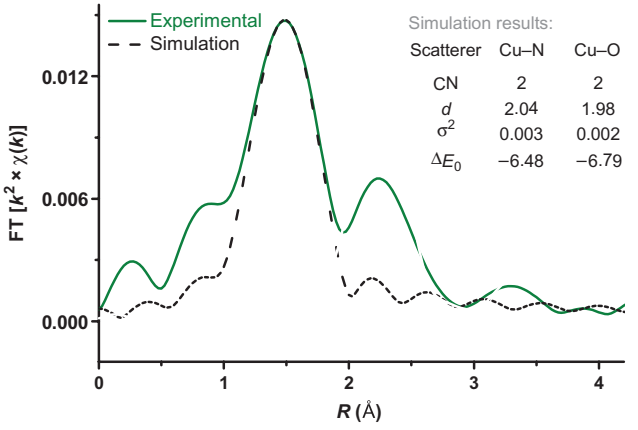

Fig. 5. The mixture of CuI, LiCl, 2a, and DMA in the presence of air at 120°C for 5 min [green line, FT (Fourier transform) = 2.62 to 9.42 Å^{-1}] and simulation (black line, fitting range = 1.09 to 1.84 Å). CN, coordination number, *d*, bond distance.

obtained fitting parameters revealed that the Cu(II) center was coordinated by two N atoms at a distance of 2.04 Å and two O atoms at a shorter distance of 1.98 Å. Additionally, no Cu–Cu scattering peak was found in the raw EXAFS data, whereas the second shell might be attributed to the Cu–C at long distance (*64*). These results indicated that the Cu(II) species should be a monomer. Therefore, we propose the structure of the Cu(II) species to be similar to **5** or **6.** However, only a small amount of the desired product was produced when $Cu(OH)_2$, instead of CuI, was used as the catalyst in this transformation (see table S1), suggesting that **5** rather than **6** might be the right structure.

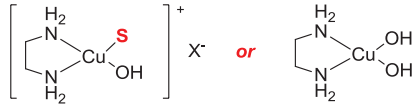

5 S = DMA or H_2O **6**

According to the design in Scheme 2, the intramolecular cyclization of the enamine cationic radical should be the key step for the formation of pyrazine. Therefore, the DFT method B3LYP was also used to study this step (*49*). On the basis of the experimental results above, the copper(II)-involved cationic radical nucleophilic addition has also been considered in Fig. 6A. The transformation starts from complex **VII** and then the cyclization product **IX** could be generated through transition state **VIII-ts** with an activation energy of 16.4 kcal/mol. Cationic radical **IX** owns two resonance structures, which are described

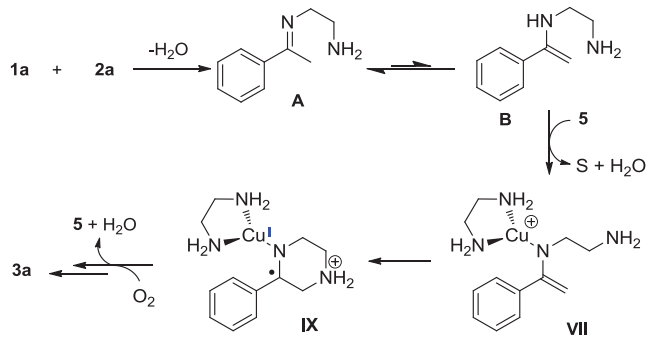

Scheme 4. Putative mechanism.

as structures **IX** and **X.** To confirm the structure of **X**, an ESP map has been calculated. The dark blue color around the nitrogen atom in Fig. 6B suggests that most of the positive charge is located on nitrogen, rather than on copper. The spin density map also indicates that minimal unpaired electron density is located on copper, whereas most of the unpaired electron is shared by nitrogen and four carbon atoms (Fig. 6C). Therefore, the cyclization product prefers to exist in the form of structure **IX.**

On the basis of the results of mechanistic investigations and DFT calculations, a putative and simplified reaction pathway was proposed for these copper-catalyzed oxidative coupling reactions (Scheme 4). Initially, condensation between acetophenone and ethylenediamine occurred to afford imine **A**, which could isomerize to enamine **B.** In the presence of Cu species **5**, the intermediate **B** turned to the **VII** species via a well-known process. Subsequently, intramolecular cyclization of intermediate **VII** occurs by way of a radical pathway. Finally, the desired pyrazine was produced along with further oxidative dehydrogenation.

CONCLUSION

In conclusion, we have developed a copper-catalyzed aerobic oxidative C–H/N–H coupling of ketones with diamines to construct aromatic pyrazine derivatives. By utilizing simple CuI as the catalyst and O_2 as the oxidant, various substituted ketones were suitable for this transformation. Compared with the traditional pyrazine syntheses from diketones with diamines, this protocol provided a more attractive approach. Preliminary mechanistic investigations indicated that radical species were involved in the transformation. Moreover, a structure of the reactive catalyst intermediate was proposed according to the XAFS experimental results. DFT calculations suggested that the intramolecular coupling of cationic radicals was a favorable pathway for this transformation. On the basis of the current mechanistic investigations, a simplified mechanism was proposed, which could be helpful for understanding the copper-catalyzed aerobic reactions. Further detailed mechanistic studies are under way in our laboratory and will be reported in the future.

MATERIALS AND METHODS

General procedure

CuI (9.5 mg, 0.05 mmol) and LiCl (42 mg, 1.0 mmol) were added to an oven-dried Schlenk tube that was then sealed with septa and fitted with an oxygen balloon. Subsequently, DMA (1 ml), ketone (0.5 mmol), Et_3N (0.5 ml), and diamine (2.5 mmol) were injected via a syringe or

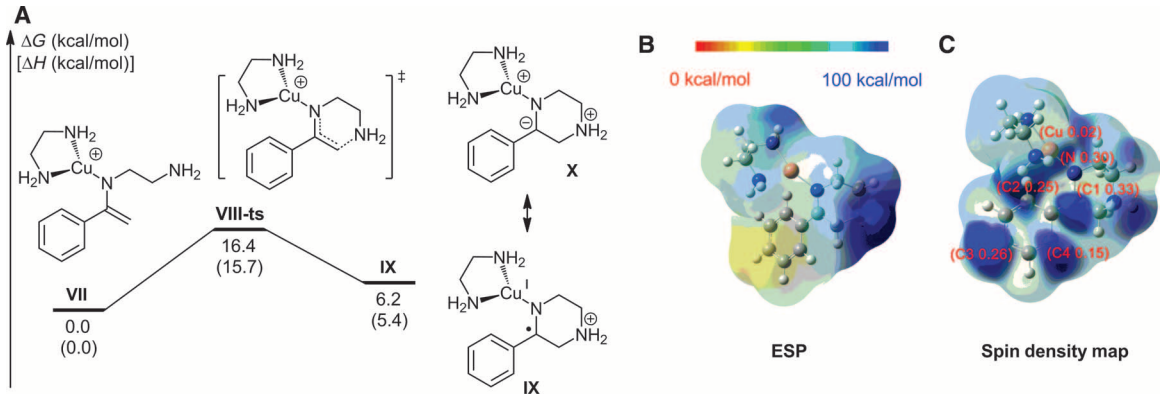

Fig. 6. Density functional theory (DFT) calculations for intramolecular cyclization of the enamine cationic radical. (**A**) Free energy profile for copper(II)-involved cyclization. (**B**) ESP map of complex **IX.** (**C**) Spin density map of complex **IX.** The numbers in parentheses are the corresponding Mulliken spin density located on each atom.

microsyringe. Finally, the Schlenk tube was allowed to stir at 120°C for 15 hours. After completion of the reaction, it was quenched by water and extracted with ethyl ether (3 × 10 ml). The organic layers were combined and dried over sodium sulfate. The pure product was obtained by flash column chromatography on silica gel (petroleum ether/ethyl acetate, 100:1).

SUPPLEMENTARY MATERIALS

Supplementary material for this article is available at http://advances.sciencemag.org/cgi/content/full/1/9/e1500656/DC1

General information
General procedure
Table S1. The evaluation of several metal salts.
Table S2. The effects of other solvents.
Table S3. The effects of reaction temperature.
Table S4. The effects of the ratio of substrates.
Table S5. The effects of LiCl loading.
Table S6. Oxidative C–H/N–H coupling between ketone and ethylenediamine under standard reaction conditions.
Scheme S1. Gas chromatography–mass spectrometry analysis of the reaction between **1a** and **2a.**
Scheme S2. Gas chromatography–mass spectrometry analysis of the reaction between **1a** and **2e.**
EPR experiments
Radical trapping experiments
Scheme S3. Radical trapping experiment using BHT [2,6-bis(1,1-dimethylethyl)-4-methylphenol] as the scavenger.
Scheme S4. Radical trapping experiment using TEMPO (2,2,6,6-tetramethylpiperidinyloxy) as the scavenger.
XAS experiments
General computational calculation details
Detailed descriptions for products
NMR data
References (*65*–*73*)

REFERENCES AND NOTES

1. C.-L. Sun, B.-J. Li, Z.-J. Shi, Pd-catalyzed oxidative coupling with organometallic reagents *via* C–H activation. *Chem. Commun.* **46**, 677–685 (2010).
2. C. Liu, H. Zhang, W. Shi, A. Lei, Bond formations between two nucleophiles: Transition metal catalyzed oxidative cross-coupling reactions. *Chem. Rev.* **111**, 1780–1824 (2011).
3. W. Shi, C. Liu, A. Lei, Transition-metal catalyzed oxidative cross-coupling reactions to form C–C bonds involving organometallic reagents as nucleophiles. *Chem. Soc. Rev.* **40**, 2761–2776 (2011).
4. G. J. Hutchings, M. S. Scurrell, J. R. Woodhouse, Oxidative coupling of methane using oxide catalysts. *Chem. Soc. Rev.* **18**, 251–283 (1989).
5. C.-J. Li, Cross-Dehydrogenative coupling (CDC): Exploring C–C bond formations beyond functional group transformations. *Acc. Chem. Res.* **42**, 335–344 (2009).
6. X. Chen, K. M. Engle, D.-H. Wang, J.-Q. Yu, Palladium(II)-catalyzed C–H activation/C–C cross-coupling reactions: Versatility and practicality. *Angew. Chem. Int. Ed.* **48**, 5094–5115 (2009).
7. C. S. Yeung, V. M. Dong, Catalytic dehydrogenative cross-coupling: Forming carbon–carbon bonds by oxidizing two carbon–hydrogen bonds. *Chem. Rev.* **111**, 1215–1292 (2011).
8. S. H. Cho, J. Y. Kim, J. Kwak, S. Chang, Recent advances in the transition metal-catalyzed twofold oxidative C–H bond activation strategy for C–C and C–N bond formation. *Chem. Soc. Rev.* **40**, 5068–5083 (2011).
9. R. Giri, B.-F. Shi, K. M. Engle, N. Maugel, J.-Q. Yu, Transition metal-catalyzed C–H activation reactions: Diastereoselectivity and enantioselectivity. *Chem. Soc. Rev.* **38**, 3242–3272 (2009).
10. T. W. Lyons, M. S. Sanford, Palladium-catalyzed ligand-directed C–H functionalization reactions. *Chem. Rev.* **110**, 1147–1169 (2010).
11. G. Dyker, *Handbook of C–H Transformations. Applications in Organic Synthesis* (Wiley-VCH, Weinheim, Germany, 2005).
12. T. Hamada, X. Ye, S. S. Stahl, Copper-catalyzed aerobic oxidative amidation of terminal alkynes: Efficient synthesis of snamides. *J. Am. Chem. Soc.* **130**, 833–835 (2008).
13. L. V. Desai, H. A. Malik, M. S. Sanford, Oxone as an inexpensive, safe, and environmentally benign oxidant for C–H bond oxygenation. *Org. Lett.* **8**, 1141–1144 (2006).
14. N. Sato, *Comprehensive Heterocyclic Chemistry II* (Pergamon, Oxford, UK, 1996).
15. S. Berg, M. Bergh, S. Hellberg, K. Högdin, Y. Lo-Alfredsson, P. Söderman, S. von Berg, T. Weigelt, M. Ormo, Y. Xue, J. Tucker, J. Neelissen, E. Jerning, Y. Nilsson, R. Bhat, Discovery of novel potent and highly selective glycogen synthase kinase-3β (GSK3β) inhibitors for Alzheimer's disease: Design, synthesis, and characterization of pyrazines. *J. Med. Chem.* **55**, 9107–9119 (2012).
16. A. Gazit, H. App, G. McMahon, J. Chen, A. Levitzki, F. D. Bohmer, Tyrphostins. 5. Potent inhibitors of platelet-derived growth factor receptor tyrosine kinase: Structure–activity relationships in quinoxalines, quinolines, and indole tyrphostins. *J. Med. Chem.* **39**, 2170–2177 (1996).
17. L. E. Seitz, W. J. Suling, R. C. Reynolds, Synthesis and antimycobacterial activity of pyrazine and quinoxaline derivatives. *J. Med. Chem.* **45**, 5604–5606 (2002).
18. S. Yanagisawa, K. Ueda, T. Taniguchi, K. Itami, Potassium *t*-butoxide alone can promote the biaryl coupling of electron-deficient nitrogen heterocycles and haloarenes. *Org. Lett.* **10**, 4673–4676 (2008).
19. S. Achelle, C. Baudequin, N. Plé, Luminescent materials incorporating pyrazine or quinoxaline moieties. *Dyes Pigm.* **98**, 575–600 (2013).
20. S. A. Raw, C. D. Wilfred, R. J. K. Taylor, Preparation of quinoxalines, dihydropyrazines, pyrazines and piperazines using tandem oxidation processes. *Chem. Commun.* **39**, 2286–2287 (2003).
21. S. A. Kotharkar, D. B. Shinde, $Pb(NO_3)_2$ mediated synthesis of pyrazine. *Chin. J. Chem.* **25**, 105–107 (2007).
22. P. Ghosh, A. Mandal, Greener approach toward one pot route to pyrazine synthesis. *Green Chem. Lett. Rev.* **5**, 127–134 (2012).
23. T.-Q. Huang, W.-Y. Qu, J.-C. Ding, M.-C. Liu, H.-Y. Wu, J.-X. Chen, Catalyst-free protocol for the synthesis of quinoxalines and pyrazines in PEG. *J. Heterocycl. Chem.* **50**, 293–297 (2013).
24. P. J. Steel, G. B. Caygill, Cyclometallated compounds V. Double cyclopalladation of diphenyl pyrazines and related ligands. *J. Organomet. Chem.* **395**, 359–373 (1990).
25. S. A. Raw, C. D. Wilfred, R. J. K. Taylor, Tandem oxidation processes for the preparation of nitrogen-containing heteroaromatic and heterocyclic compounds. *Org. Biomol. Chem.* **2**, 788–796 (2004).
26. Z. Zheng, X. Zhou, Metal-free oxidation of α-hydroxy ketones to 1,2-diketones catalyzed by mesoporous carbon nitride with visible light. *Chin. J. Chem.* **30**, 1683–1686 (2012).
27. C. Qi, H. Jiang, L. Huang, Z. Chen, H. Chen, DABCO-catalyzed oxidation of deoxybenzoins to benzils with air and one-pot synthesis of quinoxalines. *Synthesis* **2011**, 387–396 (2010).

28. A. Gao, F. Yang, J. Li, Y. Wu, Pd/Cu-catalyzed oxidation of alkynes into 1,2-diketones using DMSO as the oxidant. *Tetrahedron* **68**, 4950–4954 (2012).
29. A. K. Bagdi, M. Rahman, S. Santra, A. Majee, A. Hajra, Copper-catalyzed synthesis of imidazo[1,2-*a*]pyridines through tandem imine formation-oxidative cyclization under ambient air: One-step synthesis of zolimidine on a gram-scale. *Adv. Synth. Catal.* **355**, 1741–1747 (2013).
30. Z.-J. Cai, S.-Y. Wang, S.-J. Ji, Copper(I) iodide/boron trifluoride etherate-cocatalyzed aerobic dehydrogenative reactions applied in the synthesis of substituted heteroaromatic imidazo[1,2-*a*]pyridines. *Adv. Synth. Catal.* **355**, 2686–2692 (2013).
31. Y. Cui, C. He, A silver-catalyzed intramolecular amidation of saturated C–H bonds. *Angew. Chem. Int. Ed.* **43**, 4210–4212 (2004).
32. H. M. L. Davies, M. S. Long, Recent advances in catalytic intramolecular C–H aminations. *Angew. Chem. Int. Ed.* **44**, 3518–3520 (2005).
33. F. Collet, R. H. Dodd, P. Dauban, Catalytic C-H amination: Recent progress and future directions. *Chem. Commun.* **45**, 5061–5074 (2009).
34. C. G. Espino, P. M. Wehn, J. Chow, J. Du Bois, Synthesis of 1,3-difunctionalized amine derivatives through selective C–H bond oxidation. *J. Am. Chem. Soc.* **123**, 6935–6936 (2001).
35. X. Liu, Y. Zhang, L. Wang, H. Fu, Y. Jiang, Y. Zhao, General and efficient copper-catalyzed amidation of saturated C–H bonds using *N*-halosuccinimides as the oxidants. *J. Org. Chem.* **73**, 6207–6212 (2008).
36. G. Pelletier, D. A. Powell, Copper-catalyzed amidation of allylic and benzylic C–H bonds. *Org. Lett.* **8**, 6031 (2006).
37. R. W. Evans, J. R. Zbieg, S. Zhu, W. Li, D. W. C. MacMillan, Simple catalytic mechanism for the direct coupling of α-carbonyls with functionalized amines: A one-step synthesis of plavix. *J. Am. Chem. Soc.* **135**, 16074–16077 (2013).
38. X. Xu, Y. Deng, X. Li, Z. Zhao, W. Fang, X. Yan, Iodine (III)-mediated one-pot synthesis of quinoxaline by tandem nucleophilic substitution and cyclisation. *J. Chem. Res.* **35**, 605–607 (2011).
39. Z.-J. Cai, S.-Y. Wang, S.-J. Ji, CuI/BF_3·Et_2O cocatalyzed aerobic dehydrogenative reactions of ketones with benzylamines: Facile synthesis of substituted imidazoles. *Org. Lett.* **14**, 6068–6071 (2012).
40. M.-Y. Chang, T.-W. Lee, R.-T. Hsu, T.-L. Yen, Synthesis of quinoxaline analogues. *Synthesis* **2011**, 3143–3151 (2011).
41. M. Lian, Q. Li, Y. Zhu, G. Yin, A. Wu, Logic design and synthesis of quinoxalines via the integration of iodination/oxidation/cyclization sequences from ketones and 1,2-diamines. *Tetrahedron* **68**, 9598–9605 (2012).
42. S. E. Allen, R. R. Walvoord, R. Padilla-Salinas, M. C. Kozlowski, Aerobic copper-catalyzed organic reactions. *Chem. Rev.* **113**, 6234–6458 (2013).
43. R. Shi, L. Lu, H. Zhang, B. Chen, Y. Sha, C. Liu, A. Lei, Palladium/copper-catalyzed oxidative C–H alkenylation/N-dealkylative carbonylation of tertiary anilines. *Angew. Chem. Int. Ed.* **52**, 10582–10585 (2013).
44. J. Ke, C. He, H. Liu, M. Li, A. Lei, Oxidative cross-coupling/cyclization to build polysubstituted pyrroles from terminal alkynes and β-enamino esters. *Chem. Commun.* **49**, 7549–7551 (2013).
45. Z. Li, C.-J. Li, Highly efficient copper-catalyzed nitro-mannich type reaction: Cross-dehydrogenative-coupling between sp^3 C–H bond and sp^3 C–H bond. *J. Am. Chem. Soc.* **127**, 3672–3673 (2005).
46. T. D. Beeson, A. Mastracchio, J.-B. Hong, K. Ashton, D. W. C. MacMillan, Enantioselective organocatalysis using SOMO activation. *Science* **316**, 582–585 (2007).
47. S.-I. Murahashi, N. Komiya, H. Terai, Ruthenium-catalyzed oxidative cyanation of tertiary amines with hydrogen peroxide and sodium cyanide. *Angew. Chem. Int. Ed.* **44**, 6931–6933 (2005).
48. C. Wei, C.-J. Li, Enantioselective direct-addition of terminal alkynes to imines catalyzed by copper(I)pybox complex in water and in toluene. *J. Am. Chem. Soc.* **124**, 5638–5639 (2002).
49. Computational details are listed in the Supporting Information.
50. M. Nishino, K. Hirano, T. Satoh, M. Miura, Copper-catalyzed oxidative direct cyclization of *N*-methylanilines with electron-deficient alkenes using molecular oxygen. *J. Org. Chem.* **76**, 6447–6451 (2011).
51. G. Rossé, J. Strickler, M. Patek, Efficient solid-phase synthesis of disubstituted 1,3-dihydro-imidazol-2-ones. *Synlett* **2004**, 2167–2168 (2004).
52. I. Caretti, E. Carter, I. A. Fallis, D. M. Murphy, S. Van Doorslaer, Interactions of an asymmetric amine with a non-C_2 symmetric Cu–salen complex: An EPR/ENDOR and HYSCORE investigation. *Phys. Chem. Chem. Phys.* **13**, 20427–20434 (2011).
53. P. Håkansson, T. Nguyen, P. B. Nair, R. Edge, E. Stulz, Cu(II)-porphyrin molecular dynamics as seen in a novel EPR/Stochastic Liouville equation study. *Phys. Chem. Chem. Phys.* **15**, 10930–10941 (2013).
54. A. Samuni, C. M. Krishna, P. Riesz, E. Finkelstein, A. Russo, Superoxide reaction with nitroxide spin-adducts. *Free Radic. Biol. Med.* **6**, 141–148 (1989).
55. H. Zhao, J. Joseph, H. Zhang, H. Karoui, B. Kalyanaraman, Synthesis and biochemical applications of a solid cyclic nitrone spin trap: A relatively superior trap for detecting superoxide anions and glutathiyl radicals. *Free Radic. Biol. Med.* **31**, 599–606 (2001).
56. C. Zhang, P. Feng, N. Jiao, Cu-catalyzed esterification reaction via aerobic oxygenation and C–C bond cleavage: An approach to α-ketoesters. *J. Am. Chem. Soc.* **135**, 15257–15262 (2013).
57. R. Bai, G. Zhang, H. Yi, Z. Huang, X. Qi, C. Liu, J. T. Miller, A. J. Kropf, E. E. Bunel, Y. Lan, A. Lei, Cu(II)–Cu(I) synergistic cooperation to lead the alkyne C–H activation. *J. Am. Chem. Soc.* **136**, 16760–16763 (2014).
58. G. Zhang, H. Yi, G. Zhang, Y. Deng, R. Bai, H. Zhang, J. T. Miller, A. J. Kropf, E. E. Bunel, A. Lei, Direct observation of reduction of Cu(II) to Cu(I) by terminal alkynes. *J. Am. Chem. Soc.* **136**, 924–926 (2014).
59. A. N. Campbell, S. S. Stahl, Overcoming the "Oxidant Problem": Strategies to use O_2 as the oxidant in organometallic C–H oxidation reactions catalyzed by Pd (and Cu). *Acc. Chem. Res.* **45**, 851–863 (2012).
60. S. D. McCann, S. S. Stahl, Copper-catalyzed aerobic oxidations of organic molecules: Pathways for two-electron oxidation with a four-electron oxidant and a one-electron redox-active catalyst. *Acc. Chem. Res.* **48**, 1756–1766 (2015).
61. A. E. Wendlandt, A. M. Suess, S. S. Stahl, Copper-catalyzed aerobic oxidative C–H functionalizations: Trends and mechanistic insights. *Angew. Chem. Int. Ed.* **50**, 11062–11087 (2011).
62. A. E. King, L. M. Huffman, A. Casitas, M. Costas, X. Ribas, S. S. Stahl, Copper-catalyzed aerobic oxidative functionalization of an arene C–H bond: Evidence for an aryl-copper(III) intermediate. *J. Am. Chem. Soc.* **132**, 12068–12073 (2010).
63. A. M. Suess, M. Z. Ertem, C. J. Cramer, S. S. Stahl, Divergence between organometallic and single-electron-transfer mechanisms in copper(II)-mediated aerobic C–H oxidation. *J. Am. Chem. Soc.* **135**, 9797–9804 (2013).
64. M. Tromp, G. P. F. van Strijdonck, S. S. van Berkel, A. van den Hoogenband, M. C. Feiters, B. de Bruin, S. G. Fiddy, A. M. J. van der Eerden, J. A. van Bokhoven, P. W. N. M. van Leeuwen, D. C. Koningsberger, Multitechnique approach to reveal the mechanism of copper(II)-catalyzed arylation reactions. *Organometallics* **29**, 3085–3097 (2010).
65. A. D. Becke, Density-functional thermochemistry. III. The role of exact exchange. *J. Chem. Phys.* **98**, 5648 (1993).
66. C. Lee, W. Yang, R. G. Parr, Development of the Colle-Salvetti correlation-energy formula into a functional of the electron density. *Phys. Rev. B Condens Matter* **37**, 785 (1988).
67. S. Miertuš, E. Scrocco, J. Tomasi, Electrostatic interaction of a solute with a continuum. A direct utilization of ab initio molecular potentials for the prevision of solvent effects. *Chem. Phys.* **55**, 117–129 (1981).
68. S. Miertuš, J. Tomasi, Approximate evaluations of the electrostatic free energy and internal energy changes in solution processes. *Chem. Phys.* **65**, 239–245 (1982).
69. P. P. Singh, S. K. Aithagani, M. Yadav, V. P. Singh, R. A. Vishwakarma, Iron-catalyzed cross-coupling of electron-deficient heterocycles and quinone with organoboron species via innate C–H functionalization: Application in total synthesis of pyrazine alkaloid botryllazine A. *J. Org. Chem.* **78**, 2639–2648 (2013).
70. C. F. Harris, D. Ravindranathan, S. Huo, Oxidative addition of heteroaromatic halides to Negishi reagent and subsequent cross-coupling reactions. *Tetrahedron Lett.* **53**, 5389–5392 (2012).
71. M. Li, R. Hua, Gold(I)-catalyzed direct C–H arylation of pyrazine and pyridine with aryl bromides. *Tetrahedron Lett.* **50**, 1478–1481 (2009).
72. C.-L. Deng, S.-M. Guo, Y.-X. Xie, J.-H. Li, Mild and ligand-free palladium-catalyzed cross-couplings between aryl halides and arylboronic acids for the synthesis of biaryls and heterocycle-containing biaryls. *Eur. J. Org. Chem.* **2007**, 1457–1462 (2007).
73. R. J. Bergeron, P. Hoffman, Application of *N*-phenyltrifluoromethanesulfonamides to the synthesis of pyrazines. *J. Org. Chem.* **45**, 161–163 (1980).

Funding: This work was supported by the 973 Program (grants 2012CB725302 and 2011CB808600), the National Natural Science Foundation of China (grants 21390400, 21272180, 21302148, 21372266, and 51302327), the Research Fund for the Doctoral Program of Higher Education of China (grant 20120141130002), the Program for Changjiang Scholars and Innovative Research Team in University (grant IRT1030), and the Ministry of Science and Technology of China (grant 2012YQ120060). The Program of Introducing Talents of Discipline to Universities of China (111 Program) is also appreciated. This work was also funded by the Chemical Sciences and Engineering Division, Argonne National Laboratory. Use of the Advanced Photon Source was supported by the U.S. Department of Energy, Office of Science, Office of Basic Energy Sciences, under contract no. DE-AC02-06CH11357. MRCAT (Materials Research Collaborative Access Team) operations are supported by the Department of Energy and the MRCAT member institutions. Part of XAFS data were collected at beamline 17C1 of the National Synchrotron Radiation Research Center, Taiwan. **Author contributions:** A.L. conceived the project. K.W. and Z.H. designed and performed the synthetic work, and designed the work for mechanistic investigation. X.Q., Y. Li, and Y. Lan performed the DFT calculations. Z.H., G.Z., J.T.M., C.-W.P., and J.-F.L. performed the XAS experiments. C.L., L.M., Y. Lan, and E.E.B. discussed the results and designed part of the experiments. K.W. and H.Y. performed the EPR experiments. K.W., Z.H., and A.L. wrote the manuscript. K.W. and Z.H. wrote the supplementary materials and contributed other related materials. **Competing interests:** The authors declare that they have no competing interests. **Data and materials availabilty:** Data will be made available upon request by emailing aiwenlei@whu.edu.cn.

Submitted 21 May 2015
Accepted 22 July 2015
Published 9 October 2015
10.1126/sciadv.1500656

Citation: K. Wu, Z. Huang, X. Qi, Y. Li, G. Zhang, C. Liu, H. Yi, L. Meng, E. E. Bunel, J. T. Miller, C.-W. Pao, J.-F. Lee, Y. Lan, A. Lei, Copper-catalyzed aerobic oxidative coupling: From ketone and diamine to pyrazine. *Sci. Adv.* **1**, e1500656 (2015).